

**Key Points:**

- As probed by Huygens, the meteorological conditions near the surface of Saturn's moon Titan appear conducive to dust devil formation
- Dust devils may contribute significantly to Titan's aeolian cycle
- If dust devils are active on Titan, NASA's upcoming Dragonfly mission is likely to encounter them

Correspondence to:

B. Jackson,
bjackson@boisestate.edu

Citation:

Jackson, B., Lorenz, R. D., Barnes, J. W., & Szurgot, M. (2020). Dust devils on Titan. *Journal of Geophysical Research: Planets*, 125, e2019JE006238. <https://doi.org/10.1029/2019JE006238>

Received 7 OCT 2019

Accepted 6 FEB 2020

Author Contributions

Conceptualization: Ralph D. Lorenz, Jason W. Barnes, Michelle Szurgot

Methodology: Ralph D. Lorenz, Michelle Szurgot

Writing - Original Draft: Ralph D. Lorenz, Jason W. Barnes, Michelle Szurgot

Dust Devils on Titan

Brian Jackson¹ , Ralph D. Lorenz² , Jason W. Barnes³ , and Michelle Szurgot¹

¹Department of Physics, Boise State University, Boise, ID, USA, ²Applied Physics Laboratory, Johns Hopkins University, Laurel, MD, USA, ³Department of Physics, University of Idaho, Moscow, ID, USA

Abstract Conditions on Saturn's moon Titan suggest that dust devils, which are convective, dust-laden plumes, may be active. Although the exact nature of dust on Titan is unclear, previous observations confirm an active aeolian cycle, and dust devils may play an important role in Titan's aeolian cycle, possibly contributing to regional transport of dust and even production of sand grains. The Dragonfly mission to Titan will document dust devil and convective vortex activity and thereby provide a new window into these features, and our analysis shows that associated winds are likely to be modest and pose no hazard to the mission.

Plain Language Summary Saturn's moon Titan may host active dust devils, small dust-laden plumes, which could significantly contribute to transport of dust in that moon's atmosphere. Although the exact nature of dust on Titan is unclear, previous observations confirm that there is actively blowing dust on that world. If dust devils are active on Titan's surface, NASA's upcoming Dragonfly mission is likely to encounter them, but dust devils on Titan are unlikely to pose a hazard to the mission.

1. Introduction

Saturn's moon Titan is the only satellite in our solar system with a significant atmosphere—consisting primarily of nitrogen, the atmosphere has a surface pressure 50% larger than Earth's (Fulchignoni et al., 2005). Titan also exhibits active hydrology, resulting in Earth-like river channels, gorges, and even lakes (Hayes et al., 2018), and the Cassini Mission orbiting Saturn from 2004 to 2017 observed large, vigorous convective storms (Turtle et al., 2011). At Titan's temperatures, water forms the bedrock, while atmospheric methane and ethane act as condensables. Titan's atmosphere is also laden with organic aerosols, produced high into the thermosphere by photolysis of N₂ and CH₄ and recombination into long hydrocarbon chains. These aerosols slowly settle out onto Titan's surface at a rate of about 10⁻⁷ kg m⁻² s⁻¹ (Larson et al., 2014).

Titan also exhibits active aeolian processes. Cassini's instruments observed fields of giant sand dunes girding Titan's equator and covering about 13% of its surface (Radebaugh et al., 2008). How the dune sands, with expected grain diameters $D_p \sim 200 \mu\text{m}$ (Barnes et al., 2015), and dust grains, with diameters $D_p \sim 5 \mu\text{m}$ (Rodriguez et al., 2018), are produced is unclear, but their organic composition probably ultimately derives from the atmospheric aerosols (Barnes et al., 2015). Cassini's Visual and Infrared Mapping Spectrometer also revealed three regional dust storms near the equator (Rodriguez et al., 2018) that occurred during the equinox season in 2009. Radiative transfer modeling implicate dust grains about 5 μm in radius and resembling the organic haze in composition (Rodriguez et al., 2018). General circulation models (GCMs) of Titan predict precipitation at low latitudes during this season as the result of seasonal convergence of Hadley cells (Lora et al., 2019). The strong winds associated with this seasonal precipitation likely drive the dust storms at these low latitudes where the dune fields reside.

The dust storms' appearance not only confirms an active dust cycle, but they also suggest the possibility of other dust-lifting phenomena. Among the most ephemeral but frequent such processes on other worlds are convective, dust-laden vortices, called dust devils. Dust devils occur throughout arid regions on Earth, where they contribute to poor air quality (Gillette & Sinclair, 1990), and ubiquitously on Mars, where they may pose a hazard for human exploration (Balme & Greeley, 2006). While dust devils observations go back millennia (Lorenz et al., 2016), our understanding of their operation and how they lift dust remains poor. If dust devils do exist on Titan, the unique aerodynamic environment may provide an unparalleled window into dust devil physics.

The recently selected Dragonfly mission could serve to elucidate dust devil processes through extended observation on the ground (rather like Mars landers). Dragonfly is a rotorcraft lander that will fly on Titan

©2020. The Authors.

This is an open access article under the terms of the Creative Commons Attribution License, which permits use, distribution and reproduction in any medium, provided the original work is properly cited.

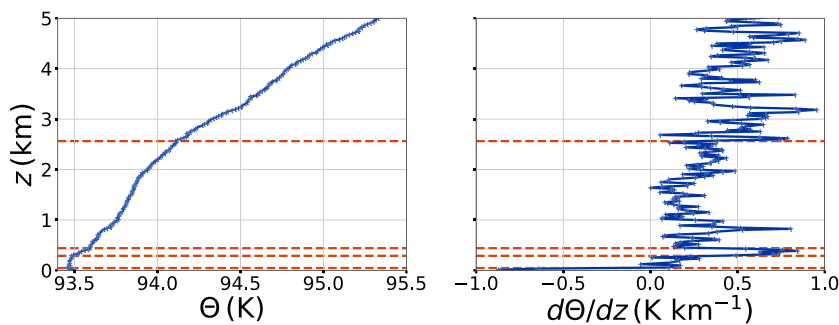


Figure 1. Titan's potential temperature profile and its derivative. The left panel shows the inferred potential temperature profile Θ (blue) in degrees Kelvin as a function of altitude z in kilometers, while the right panel shows the derivative. The dashed orange lines indicate statistically significant kinks in the Θ profile, possibly corresponding to boundary layer features.

to explore that world's potential habitability and study its complex methane cycle. Titan's thick atmosphere and low gravity facilitate flight, motivating proposals to explore Titan by air for two decades (Barnes et al., 2012; Lorenz, 2000; Spilker, 2005). The Dragonfly mission was selected for launch in 2026 and arrival at Titan by 2034 (Lorenz et al., 2018) and will fly over Titan's equatorial sand seas and characterize the chemical, geophysical, meteorological, and aeolian environment (Rafkin et al., 2018). As we argue here, dust devils may stalk these very dunes, and so Dragonfly is likely to encounter active dust devils, most while landed, allowing us to probe their structures.

For this study, we focus on meteorological conditions near Titan's equator, where sand dunes and dust storms have been observed. Although dust devils may occur elsewhere on Titan and, as we argue, may contribute to global dust transport, the lack of near-surface data for other latitudes precludes a more comprehensive analysis. In addition, many of the relationships used throughout this study apply to convective vortices in general, not just dust devils. Of particular importance, equation (4) used to assess dust devil frequency considers all convective plumes, not just dust devils. We argue that winds in some vortices are likely sufficient to loft dust, and we attempt to account for dustless vortices. However, such vortices very likely occur alongside dust devils on Titan, if either occurs, and the relative occurrence rates are unclear. This is a key uncertainty in our study and may be addressed by the Dragonfly mission.

2. Properties of Dust Devils on Titan

Titan's meteorological conditions determine convective vortex and dust devil occurrence and properties (wind speeds, sizes, occurrence frequency, etc.). Several analytic and empirical criteria have been developed to relate these conditions to vortex and dust devil properties. The structure of the planetary boundary layer plays a key role, and it was probed at high resolution by the Huygens probe on 14 January 2005 at 09:47 local solar time (Cousstenis et al., 2010). Figure 1 shows the potential temperature profile Θ calculated from Huygens measurements (Tokano et al., 2006) of the actual temperature T and atmospheric pressure $P(z)$ as $\Theta = T[P(z)/P_{\text{bot}}]^{\chi}$, where P_{bot} is the atmospheric pressure at the bottom of the atmosphere (1,470 hPa), and χ is the ratio of the specific gas constant to the specific heat capacity at fixed pressure, 0.3108 (Tokano et al., 2006). We explored this profile for boundary layer structures by calculating an altitude derivative and applying a first-order Savitzky-Golay filter (Savitzky & Golay, 1964) and a window size of three points (i.e., we fit a piecewise first-order polynomial, three points at a time) to moderately smooth the derivative. Otherwise, statistically insignificant excursions in the derivative would hamper our search for robust variations. We then applied the Bayesian blocks algorithm (Scargle et al., 2013) to the derivative to search for change points, which may correspond to boundary layer depth h . Frequent convective overturn takes place in the boundary layer, which can produce a region with a uniform potential temperature (i.e., an isentropic region). Thus, a change in the potential temperature profile may reflect the top of the planetary boundary layer, as suggested by previous studies (Tokano et al., 2006).

Below 5 km altitude, we found four distinct change points at 46 m, 288 m, 440 m, and 2.6 km altitude. The lowermost change point may be the top of the surface layer (Stull, 1988), while the next two points higher up coincide closely with the top of a boundary layer previously identified at 300 m (Tokano et al., 2006) and which may diurnally deepen to 800 m (Charnay & Lebonnois, 2012). The point at 2.6 km may correspond

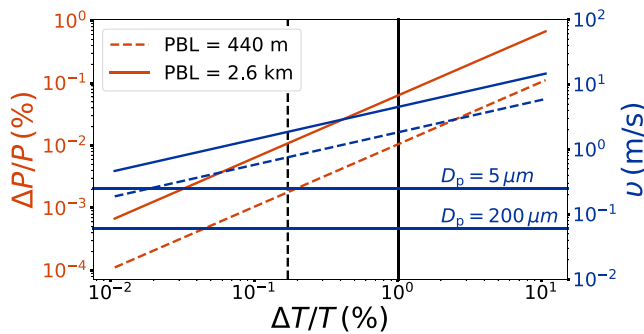


Figure 2. Dust devil pressure perturbations and wind speeds. The fractional pressure perturbations $\Delta P/P$ (orange curves) and tangential wind velocities v (blue curves) for a given temperature perturbation $\Delta T/T$ at the center of a convective vortex. The dashed lines assume a planetary boundary layer (PBL) of depth 440 m, while the solid lines assume a depth of 2.6 km. The solid, horizontal blue lines show the threshold wind speeds to initiate particle movement (Burr et al., 2015) with diameters $D_p = 5 \mu\text{m}$ (dust) and $200 \mu\text{m}$ (sand). The black vertical lines show the minimum $\Delta T/T$ given by inequality (3).

$\Delta P/\rho$, where ρ is the atmospheric density (5.3 kg m^{-3}). Figure 2 shows the expected ΔP and v for a range of ΔT . The range of ΔT that actually manifests near Titan's surface is unclear, and additional modeling and direct observation are required for an accurate assessment. In absence of such information, for our calculations, we chose a range spanning well above and below previous estimates of $\sim 1 \text{ K}$ (Tokano, 2005). The results show that for $h = 2.6 \text{ km}$ and $\Delta T/T = 1\%$ ($\Delta T = 0.9 \text{ K}$) that we expect $\Delta P/P \approx 6\%$ and $v \approx 5 \text{ m s}^{-1}$, comparable to terrestrial dust devils (Balme & Greeley, 2006).

In order to initiate a convective vortex, there must be sufficient convective energy in the boundary layer to overcome the boundary layer turbulence. Field work and theoretical analyses suggest the following criterion for dust devil formation (Rafkin et al., 2016):

$$-\frac{h}{L} > 100, \quad (2)$$

where h is the boundary layer depth and L is the Obukhov length (Obukhov, 1971). In this context, the Obukhov length is the height above the ground at which production of turbulence by shear and buoyancy are equal, and a small negative value may imply buoyant conditions (Rafkin et al., 2016). Based on the data returned by the Huygens lander (Tokano et al., 2006), L was calculated as -0.32 m , giving $-h/L \approx 1,000$ for $h = 440 \text{ m}$. Inequality (2) suggests a lower limit on $\Delta T/T$ required to form dust devils. Combining inequality (2) and the definition for L (as described in detail in Appendix A), we find

$$\frac{\Delta T}{T} > \frac{100(4f)^2}{\kappa g C_H} h = (3.9 \times 10^{-6} \text{ m}^{-1}) h, \quad (3)$$

where f is the Coriolis parameter ($1.6 \times 10^{-6} \text{ s}^{-1}$), κ the von Kármán parameter (≈ 0.4), g the gravitational acceleration (1.35 m s^{-2}), and C_H the surface heat coefficient, which is comparable to the surface drag coefficient ~ 0.002 (Arya, 1977; Tokano et al., 2006). The vertical black lines in Figure 2 show that the required variations are very modest for either value of h : less than 0.2 K for $h = 440 \text{ m}$ and about 1 K for $h = 2.6 \text{ km}$. Whether such temperature contrasts manifest over the scales relevant for convective vortex formation ($\sim 1 \text{ km}$) is unclear since sufficiently high resolution temperature measurements are unavailable. However, models (Tokano, 2005) of near-surface temperatures show that variations in surface albedo, emissivity, and/or thermal inertia can plausibly produce temperature variations $\sim 1 \text{ K}$. As a check, we applied this criterion to terrestrial dust devils. For the Earth, $f \approx 8 \times 10^{-5} \text{ s}^{-1}$, C_H near the surface is ~ 0.01 (Arya, 1977), the midday boundary layer is typically 500 m deep (Arya, 2001), requiring $\Delta T/T > 0.1$. One field study of active terrestrial dust devils (Tratt et al., 2003) found $\Delta T/T \sim 0.06$.

We can explore convective instability by considering the Richardson number Ri , defined as $Ri = (g/T)\Gamma |\partial V/\partial z|^{-2}$, where Γ is the atmospheric lapse rate, and $\partial V/\partial z$ is wind shear near the surface. A large, negative Richardson number Ri predicts convective instability (Arya, 2001). The near-surface

to the seasonally averaged boundary layer suggested in analyses of GCMs (Charnay & Lebonnois, 2012) and the morphology of Titan's equatorial dunes (Lorenz et al., 2010). For our analysis, we consider 440 m and 2.6 km for h , although it is possible the change point at 288 m also represents an atmospheric structure. Additional modeling is probably required to assess that possibility.

Dust devils can be modeled as Carnot heat engines (Rennó et al., 1998) with an efficiency η given by $\eta = (T_{\text{bot}} - T_{\text{top}})/T_{\text{bot}}$, where T_{bot} is the temperature at the surface (93.5 K as indicated by Huygens's profile) and T_{top} is the temperature at the top of the boundary layer, which we take from Huygens's profile for a given value of h . The convective pressure perturbation at its center ΔP can be calculated as

$$\Delta P = P \left(1 - \exp \left[\left(\frac{\gamma - \eta}{\gamma - \eta - 1} \right) \left(\frac{\Delta T}{T_s} / \chi \right) \right] \right), \quad (1)$$

where γ is fraction of energy lost to friction with the surface (≈ 1) and ΔT is the entropy-weighted temperature contrast between the dust devil's convective center and the surrounding surface. Cyclostrophic balance in a convective vortex gives the tangential wind speed at the eyewall as $v^2 \approx$

potential temperature lapse rate measured during Huygens's descent was $\Gamma = -0.9 \text{ K km}^{-1}$, and Doppler tracking of Huygens (Bird et al., 2005) found near-surface ($z < 660 \text{ m}$) shear of about 10 m/s/km (Lorenz, 2017). By fitting a first-order polynomial to the lowermost two points in the wind profile and considering the uncertainties, we estimate a shear of about 4 m/s/km and $Ri = -0.8$ for the time and location probed by Huygens. Although the wind shear estimate here is based on only a few measurements, higher-resolution wind profiles from GCM analyses (Lora et al., 2015) also predict a very small near-surface wind shear, which can help promote convective instability. Large eddy simulations of dust devil formation (Klose & Shao, 2016) suggest such a large and negative Richardson number corresponds to dust devil occurrence rates exceeding $1 \text{ km}^{-2} \text{ hr}^{-1}$ for Earth-like surface heating rates. Moreover, temperature and wind speed measurements made between 2 and 9 m altitude inside three active dust devils on the Earth (Sinclair, 1973) give $Ri \leq -0.4$.

Regarding the sizes of dust devils on Titan, imaging studies for the Earth and Mars suggest that dust devil diameters D are about 5 times smaller than their heights (Lorenz, 2013) and their heights are capped by the planetary boundary layer height (Fenton & Lorenz, 2015). Therefore, for $h = 2.6 \text{ km}$, $D \sim 520 \text{ m}$, and for $h = 440 \text{ m}$, $D \sim 88 \text{ m}$, small enough not to have been detected by Cassini. Regarding the smallest dust devils we might expect, the Obukhov length, $\sim 1 \text{ m}$, may set the minimum diameter for convective vortices generally (Lorenz, 2011). Our estimates for tangential velocities and diameters suggest vorticities $\zeta \approx 10^{-2} \text{ s}^{-1}$, much smaller than typical dust devils (Raasch & Franke, 2011; Rennó et al., 1998) $\geq 1 \text{ s}^{-1}$. However, since dust devils are known to span a wide range of sizes (Lorenz & Jackson, 2016), this calculation may underestimate the typical vorticity. Indeed, previous studies (Lorenz, 2011) suggest terrestrial and Martian dust devil diameters follow a power law, $\delta(D) \propto D^\alpha$, with $-2 \leq \alpha \leq -1$ (Lorenz & Jackson, 2016).

Dust devils do not involve latent heating and may, in fact, be inhibited by the presence of liquids. On Earth, wetting of the surface can suppress dust devils (Jackson & Lorenz, 2015) by increasing particle cohesion (and thus increasing the threshold wind required for dust-lifting) and surface thermal inertia, thereby damping the surface temperature response to solar heating and inhibiting boundary layer formation. Observations (Griffith et al., 2005; Schaller, Brown, Roe, & Bouchez 2006; Schaller, Brown, Roe, Bouchez, & Trujillo 2006; Turtle et al., 2011) show that large methane downpours occur on Titan, but any given spot on the surface may only see rain once every 10 Earth years (Charnay et al., 2014). Rainfall is predicted to reevaporate over a period of a few Titan years (Newman et al., 2016). Moreover, the presence of dunes (Lorenz et al., 2006) and dust storms (Rodriguez et al., 2018) near Titan's equator indicates insufficient surface wetting to totally extinguish aeolian processes. Surface humidity levels measured by Huygens were 50%, too small for cloud formation, which may require a humidity level of 60% (Griffith et al., 2000), and also too small for substantial rainfall, which may require a humidity level of 80% (Hueso & Sánchez-Lavega, 2006). Except for equinoctial (once every 16 years) outbursts at low latitudes (Lora et al., 2019; Mitchell, 2008; Newman et al., 2016), Titan's global circulation drives condensables away from the equator (Lora et al., 2015; Mitchell, 2008). Even though subsurface moisture was indicated by the Huygens instruments at its streambed landing site, the Huygens imager/spectrometer instrument detected possible dust lofted by the probe's aerodynamic wake at impact (Schröder et al., 2012). Thus, we expect arid conditions near the equator suitable for dust devil formation.

However, some conditions on Titan may impede dust devil production. The ambient wind field is probably the source for dust devil vorticity, requiring some minimum ambient wind speed; field studies (Rafkin et al., 2016) suggest 1 m s^{-1} . Whether the same threshold applies to Titan should be the subject of future work, but measured surface wind speeds (Bird et al., 2005) are $\leq 1 \text{ m s}^{-1}$, while results from (Tokano, 2010) and (Lora et al., 2015) suggest typical speeds below 0.5 m s^{-1} at low latitudes. However, higher-resolution models (and in particular large eddy simulations, which have typical resolutions of order tens of meters) may produce different results, and therefore future work should consider such models. Moreover, additional work is required to assess whether a sufficiently large fraction of surface heating on Titan partitions into sensible heating, which is required to drive convective vortex production, rather than latent heating. In other words, what is the relevant Bowen's ratio for Titan (Arya, 2001)? Titan represents a key experiment in this aspect of micrometeorology. Static charging of grains may inhibit dust mobilization—dust on Titan may develop much higher charges than terrestrial grains (Méndez Harper et al., 2017), forming approximately millimeter-sized clumps which are much larger than expected for sand grains, and so mobilization may require wind speeds a few times larger than for uncharged grains. In the end, though, the presence of active dust storms on Titan means that surface winds must occasionally mobilize dust.

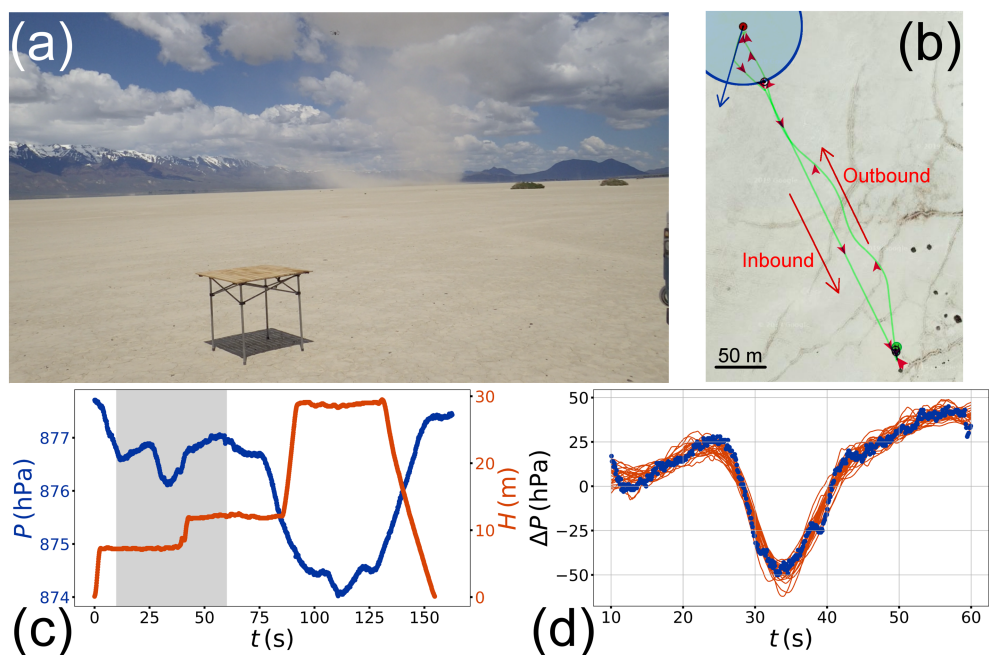


Figure 3. A dust devil encounter on the Alvord Desert in Oregon. (a) Launch of the drone (visible at top middle) toward the dust devil. (b) Drone outbound and inbound trajectories, with dust devil's approximate size (100 m) and position at encounter depicted as a blue circle. (c) Pressure P in hectopascals shown in blue and drone altitude H in meters shown in orange during the drone's flight. The gray shaded region highlights the dust devil encounter. (d) The pressure fluctuation associated with the dust devil in blue, along with model fits including a Gaussian process turbulent noise model (Jackson et al., 2018) in orange. A video of the encounter is available online (at <https://youtu.be/eOxklEkYwwE>).

What might be the significance of dust devils for Titan's meteorology and aeolian cycle? On Mars, dust devils help maintain the background atmospheric haze, which probably contributes about 10 K of radiative heating (Basu et al., 2004). Continual high-altitude production of haze means Titan's atmosphere is already loaded with aerosols, and unlike on Mars, dust devils probably do not contribute significantly to maintaining the hazy atmosphere. However, dust devils may be important for aerosol transport since surface winds are usually weak. As on Mars, dust storms on Titan probably occur infrequently near the equator, perhaps during seasonal wind storms (Rodriguez et al., 2018), but conditions may frequently allow dust devil formation. The results from lab experiments (Neakrase et al., 2006) suggest that, for a planetary boundary layer depth of 2.6 km, a terrestrial dust devil with $\Delta T/T \sim 1\%$, and therefore $\Delta P/P \sim 0.1\%$, could lift $0.025 \text{ kg m}^{-2} \text{ s}^{-1}$. Given Titan's surface pressure, such a devil would probably lift more, greatly exceeding the haze production rate of $10^{-7} \text{ kg m}^{-2} \text{ s}^{-1}$ (Larson et al., 2014). Indeed, if they occur, dust devils may be the primary mode of dust transport in arid regions on Titan. They may also raise dust grains to altitudes where regional winds can pick them up and so contribute to regional dust transport, with ultimate deposition in Titan's seas (Klose et al., 2016). Dust devils may also figure in the creation of dune sands from dust grains. Tumbling in a dust devil may charge dust grains, and such charging can result in multiparticle clumps approaching 5 mm in size (Méndez Harper et al., 2017). Whether such clumps could survive reptation and saltation involved in dune evolution is unclear, but the clumping may help initiate the sand formation process (Barnes et al., 2015). Interestingly, dust transport on Titan, where conditions may favor direct lifting of dust grains, may differ substantially from transport on Mars, where dust lifting is primarily via saltation since direct lifting on Mars requires very large wind speeds (Greeley & Iversen, 1985).

For all its similarity to Earth, Titan represents a novel regime for aeolian studies. Given the wide availability of dust and the scaling arguments presented here, even the absence of dust devils would be an important result. Probing active dust devils with an instrumented drone has been the subject of recent successful terrestrial field studies (Jackson et al., 2018) and is helping to reveal the relationships between pressure, temperature, wind, and a devil's dust-lifting capacity (Neakrase et al., 2016). Figure 3 shows results from a recent field study conducted by our group. The pressure signal registered during the dust devil encounter is

shown in panel (d). Fitting a standard Lorentzian profile (Jackson et al., 2018), we estimate $\Delta P = 80 \pm 11$ hPa, corresponding to a tangential velocity $v \approx \sqrt{80 \text{ hPa}/1 \text{ kg m}^{-3}} = 9 \text{ m s}^{-1}$. By-hand feature-tracking analysis of the encounter video collected on-board the drone confirms $v \sim 10 \text{ m s}^{-1}$. As we discuss in the next section, since Dragonfly will carry similar meteorological sensors and cameras, similar experiments can be conducted. However, since dust devils are most likely to be encountered while Dragonfly is on the ground, terrestrial (Jackson & Lorenz, 2015) and Martian (Greeley et al., 2006) fixed station studies of dust devils may be more analogous. For instance, collection of pressure and temperature time series while being passed over by a dust devil will provide their profiles (although distinguishing dust devils from dustless vortices using only pressure and temperature is difficult). Analysis of dust devil image contrast can provide estimates of dust loading (Greeley et al., 2006). In cases where dusty and dustless vortices can be distinguished, post-processing of Dragonfly's pressure time series may yield the signatures of dust devil encounters (Jackson & Lorenz, 2015) which, in turn, can provide the underlying occurrence rates (Lorenz & Jackson, 2016) and allow estimates of regional dust transport (Klose & Shao, 2016).

3. Discussion and Perspectives: The Dragonfly Mission

Given the recent selection by NASA of the Dragonfly mission to fly on Titan by 2034, we may have the opportunity to probe active dust devils in a totally novel environment. If dust devils exist on Titan, then the Dragonfly mission can provide crucial insight into how they operate. The mission will probe the chemical, geophysical, meteorological, and aeolian environment (Rafkin et al., 2018). The DraGMet geophysics and meteorology package will measure pressure, temperature, wind speed, and methane humidity, data which may elucidate structure and formation conditions for convective vortices including dust devils. DragonCam will provide panoramic imaging for navigation and may also provide images of dust devils and a microscopic imager to examine surface materials down to the scale of sand grains (MacKenzie et al., 2019), crucial for assessing aeolian processes. Using $\sim 10 \text{ km}$ and 500 m altitude flights (at $\sim 10 \text{ m s}^{-1}$ flight speed) powered by a Multi-Mission Radioisotope Thermoelectric Generator, Dragonfly will hop between equatorial interdunes to reconnoiter landing sites.

With wind speeds of a few meters per second, any convective vortex would only moderately perturb Dragonfly's flight, and, indeed, small, commercial quadcopters such as the DJI Phantom 4 (weighing 1.5 kg and spanning 50 cm) are rated to fly in wind speeds up to 11 m s^{-1} . A published estimate for Dragonfly's final mass exceeds 400 kg (Lorenz et al., 2018). As shown in Figure 2, such wind speeds would require $\Delta T/T$ in excess of 10% ($\approx 10 \text{ K}$), much larger than the 1 K seen on Titan (Cottini et al., 2012; Lora et al., 2015; Tokano, 2005). More likely, for $h = 2.6 \text{ km}$ and $\Delta T/T = 1\%$ (1 K), dust devils will exhibit $v \approx 4.5 \text{ m s}^{-1}$. Since drag scales as ρv^2 and Titan's atmospheric density is about 5 times Earth's, a 4.5 m s^{-1} wind on Titan is equivalent to a 10 m s^{-1} wind on Earth, below the threshold for much smaller commercial drones.

We can use our earlier estimates and adapt previous work to estimate the frequency of dust devil encounters for Dragonfly, both while the spacecraft is in flight and while it is on the ground. The frequency of dust devil encounters will depend on the currently unknown flight trajectories and times of day and particularly on the dust devil areal density. We can estimate this density using scalings for convective activity that have previously been applied to Titan (Lorenz et al., 2005). The fractional surface area covered by convective plumes, f , (convective plumes of all types, not just dust devils) is given by

$$f = \sqrt{\mu/\eta} (c_p \Delta T)^{-3/2} \rho^{-1} F_{in}, \quad (4)$$

where μ is the ratio of frictional dissipation to a plume's kinetic energy and is ≈ 16 (Rennó & Ingersoll, 1996). F_{in} is the surface heat flux. Plugging typical terrestrial values (Rennó et al., 1998) into equation (4) gives $f_{Earth} \approx 3 \times 10^{-3}$, but small-scale plumes such as dust devils comprise only one kind of convective system and therefore contribute only a portion of f . We can estimate the f value relevant for terrestrial dust devils by considering power law distribution of diameters (and therefore areas) and using results from in situ visual surveys of dust devils (Lorenz & Jackson, 2016) (see Appendix A). With this approach, we infer a value for f_{Earth} about 4 times smaller than the value given by equation (4). Turning to Titan, we can use the temperature profile in Figure 1 and, taking $h = 440 \text{ m}$, $\eta = 0.003$. Into equation (4) we can plug $\Delta T = 1 \text{ K}$ and $F_{in} = 1 \text{ W m}^{-2}$ (Tokano et al., 2006) and scale down by the same factor of 4 as for the Earth, giving $f_{Titan} = 10^{-4}$. We can then convert this fractional area coverage into an areal density for dust devils using

$$N = \int_{D_{min}}^{D_{max}} f_{Titan} (4/\pi) D^{-2} \delta(D) dD, \quad (5)$$

where $D_{\min/\max}$ is the minimum/maximum diameter. With $D_{\max} = 440 \text{ m}/5 = 88 \text{ m}$ and $D_{\min} = L \approx 1 \text{ m}$, $N \approx 28 \text{ km}^{-2}$.

Assuming dust devils reach Dragonfly's altitude ($\approx 500 \text{ m}$), an encounter while Dragonfly is in flight requires a devil to pass through a corridor centered on Dragonfly and running parallel to the flight path. The width of this corridor is equal to the devil's diameter; dust devils farther left or right will not register an encounter. We can estimate the mean free path between encounters for dust devils with a range of diameters as $\lambda = \int (N D)^{-1} \delta(D) dD = 13 \text{ km}$ for $\delta(D) \propto D^{-1.5}$. This result is insensitive to the exact values for the power law exponent and the minimum and maximum diameters.

Assuming that Dragonfly's ground velocity during flight, $\sim 10 \text{ m s}^{-1}$ (Lorenz et al., 2018), greatly exceeds the dust devils' velocities ($\sim 1 \text{ m s}^{-1}$), this value for λ would imply between two and three encounters during each flight. However, Dragonfly is planned to fly in the early morning, local Titan time, when conditions are calm and dust devils are probably less active. Since Dragonfly will spend most of its time on the ground, encountered dust devils will likely be carried by the ambient wind. Dust devil occurrence peaks when the surface temperature reaches a maximum (Jackson & Lorenz, 2015), and observations of Titan's diurnal surface temperatures (Cottini et al., 2012) indicate a broad peak from about 11 a.m. till 3 p.m. local time. Since Titan days are about 16 Earth days long, this time span corresponds to 64 Earth hours. In that case, Dragonfly might encounter one dust devil every 3.6 Earth hours, or nearly 20 devils while the spacecraft is on the ground each Titan day. More detailed meteorological (Newman et al., 2019) and statistical (Lorenz, 2014) modeling of predicted dust devil activity as a function of time of sol and season could improve these estimates. However, in the absence of such modeling, these estimates suggest that, if dust devils occur on Titan, Dragonfly is likely to encounter them regularly.

4. Conclusions

Meteorological conditions near the surface of Titan as probed by the Huygens lander and Cassini observations of dust storms suggest the possibility of active small-scale convective vortices including dust devils on that world. A boundary layer depth much larger than the Obhukov length scale (Rafkin et al., 2016), coupled to very low near-surface wind shear (Lorenz, 2017), is consistent with active dust devils, even though temperature variations near Titan's surface (and therefore atmospheric buoyancy) are likely to be subdued compared to Earth and Mars (Tokano, 2005).

If they exist, convective vortices including dust devils on Titan likely span a range of sizes, depending on the depth of the planetary boundary layer h during the time of day they form, with typical diameters for dust devils of either $\sim 88 \text{ m}$ (for $h = 440 \text{ m}$) or $\sim 520 \text{ m}$ (for $h = 2.6 \text{ km}$; Charnay & Lebonnois, 2012; Lorenz et al., 2010). The tangential windspeeds at the vortex eyewalls are likely to be only a few meters per second, sufficient to lift the $5 \mu\text{m}$ dust grains thought to populate Titan's dust storms (Rodriguez et al., 2018). As winds near Titan's surface probably rarely exceed 1 m s^{-1} (Cottini et al., 2012; Lora et al., 2015; Tokano, 2005), dust devils may play a key role in Titan's aeolian cycle.

Field studies using instrumented drones have helped reveal interior structures and activity within terrestrial dust devils (Jackson et al., 2018) and may provide key evidence to unravel the still-obscure physical mechanisms by which devils loft and carry dust. The arrival of NASA's Dragonfly mission on Titan in 2034 presents the prospect of probing extraterrestrial vortices in a similar way to these field studies, although encounters will probably occur primarily while Dragonfly is on the ground. However, Titan's relevant meteorological conditions suggest that vortex encounters, if in-flight, may occur a few times during Dragonfly's daily flight. The low wind speeds expected for dust devils on Titan mean they will pose little to no hazard to the mission. However, Dragonfly will spend most of its time on the ground, including during Titan's midday when vortices are most likely to be active (Jackson & Lorenz, 2015), and so encounters will probably occur on the ground every few Earth hours instead. In this case, they will likely resemble encounters on Mars by landed spacecraft. Even then, though, the imagery and meteorological data collected by Dragonfly during encounters may break new ground in aeolian studies by showing how they operate in a new aerodynamic environment.

Appendix A

Here, we derive inequality (3). It is important to note that equations (1)–(3) in the main narrative above were originally developed specifically for application to dust devils, but they may also apply to convective

vortices generally. In this Appendix, none of the equations apply uniquely to dust devils, although some of the numerical values (e.g., $R = 100 \text{ km}^{-2} \text{ day}^{-1}$) do.

To begin, inequality (3) relies on the definition of the Obukhov length, given by (Arya, 2001)

$$L = \frac{-u_*^3}{(\kappa g H) / (\bar{T} \rho c_p)}, \quad (\text{A1})$$

where u_* is the friction velocity, κ the von Kármán parameter (≈ 0.4), g the gravitational acceleration (1.35 m s^{-2}), H the surface heat flux, \bar{T} the average atmospheric temperature near the surface (93.5 K), ρ the atmospheric density at the surface (5.3 kg m^{-3}), and c_p the specific heat capacity ($1, 100 \text{ J kg}^{-1} \text{ K}^{-1}$). The friction velocity is related to the boundary layer depth via the Ekman layer approximation (Lorenz et al., 1995):

$$u_* \approx 4f h, \quad (\text{A2})$$

where f is the Coriolis parameter (Holton, 1992), which we take as $1.6 \times 10^{-6} \text{ s}^{-1}$ since Dragonfly will land near Titan's equator. We can estimate the surface heat flux as (Arya, 2001)

$$H = C_H \rho u_* c_p \Delta T_{\text{surf-air}}, \quad (\text{A3})$$

where C_H is the surface heat coefficient (Arya, 1977) and $\Delta T_{\text{surf-air}}$ is the difference in temperature between the ground and the near-surface atmosphere. Since the lateral temperature difference in the near-surface atmosphere ΔT that appears in equation (1) arises from the surface heating, we take $\Delta T \approx \Delta T_{\text{surf-air}}$. Combining all these equations, plugging them into inequality (2), and rearranging gives inequality (3).

Next, we discuss our calculation of the fractional area for terrestrial dust devils f_{Earth} . Based on several in situ visual surveys of dust devils, (Lorenz & Jackson, 2016) suggests that the dust devil occurrence rate in arid regions as integrated over all diameters is $R = 100 \text{ km}^{-2} \text{ day}^{-1}$. Therefore, the diameter power law $\delta(D)$ must satisfy

$$R = 100 \text{ km}^{-2} \text{ day}^{-1} = \int_{D_{\min}}^{D_{\max}} \delta_0 D^{-1.5} dD, \quad (\text{A4})$$

where δ_0 is the normalization constant. Taking $D_{\min} = 1 \text{ m}$ and $D_{\max} = 100 \text{ m}$ (Lorenz & Jackson, 2016) and solving this equation gives $\delta_0 \approx 0.6 \text{ km}^{-2} \text{ day}^{-1} \text{ km}^{0.5}$. The fractional area f must satisfy

$$f = \int_{D_{\min}}^{D_{\max}} \delta A \tau dD, \quad (\text{A5})$$

where A is the area of a single dust devil, $\frac{\pi}{4} D^2$. The lifetime of a dust devil τ seems to scale with diameter (Lorenz, 2013) as $\tau = (40 \text{ s}) (D/\text{m})^{2/3}$. Plugging these expressions into equation (A5) and integrating gives $f_{\text{Earth}} \approx 8.7 \times 10^{-4}$. It is important to note that visual surveys likely under-count small dust devils, those with little dust opacity, and completely miss dustless vortices.

Acknowledgments

The authors acknowledge considerable helpful input from the Editor and our referees, Jim Murphy and Claire Newman. This work was supported by Grant 80NSSC19K0542 from NASA's Solar System Workings program and by a grant from the Idaho Space Grant consortium. R. L. acknowledges the support of NASA Grants 80NSSC18K1626 (InSight PSP) and 80NSSC18K1389 (Cassini/Huygens). All data and the code to perform the calculations presented here are available (at <https://zenodo.org/record/3470280>).

References

- Arya, S. P. S. (1977). Suggested revisions to certain boundary layer parameterization schemes used in atmospheric circulation models. *Monthly Weather Review*, 105(2), 215. [https://doi.org/10.1175/1520-0493\(1977\)105h0215:SRTCBLi2.0.CO;2](https://doi.org/10.1175/1520-0493(1977)105h0215:SRTCBLi2.0.CO;2)
- Arya, S. P. (2001). *Introduction to micrometeorology*. London: Academic.
- Balme, M., & Greeley, R. (2006). Dust devils on Earth and Mars. *Reviews of Geophysics*, 44, RG3003. <https://doi.org/10.1029/2005RG000188>
- Barnes, J. W., Lemke, L., Foch, R., McKay, C. P., Beyer, R. A., Radebaugh, J., et al. (2012). AVIATR—Aerial Vehicle for In-situ and Airborne Titan Reconnaissance. A Titan airplane mission concept. *Experimental Astronomy*, 33(1), 55–127. <https://doi.org/10.1007/s10686-011-9275-9>
- Barnes, J. W., Lorenz, R. D., Radebaugh, J., Hayes, A. G., Arnold, K., & Chandler, C. (2015). Production and global transport of Titan's sand particles. *Planetary Science*, 4, 1. <https://doi.org/10.1186/s13535-015-0004-y>
- Basu, S., Richardson, M. I., & Wilson, R. J. (2004). Simulation of the Martian dust cycle with the GFDL Mars GCM. *Journal of Geophysical Research*, 109, E11006. <https://doi.org/10.1029/2004JE002243>
- Bird, M. K., Allison, M., Asmar, S. W., Atkinson, D. H., Avruch, I. M., Dutta-Roy, R., et al. (2005). The vertical profile of winds on Titan. *Nature*, 438, 800–802. <https://doi.org/10.1038/nature04060>
- Burr, D. M., Bridges, N. T., Marshall, J. R., Smith, J. K., White, B. R., & Emery, J. P. (2015). Higher-than-predicted saltation threshold wind speeds on Titan. *Nature*, 517(7532), 60–63. <https://doi.org/10.1038/nature14088>
- Charnay, B., Forget, F., Tobie, G., Sotin, C., & Wordsworth, R. (2014). Titan's past and future: 3D modeling of a pure nitrogen atmosphere and geological implications. *Icarus*, 241, 269–279. <https://doi.org/10.1016/j.icarus.2014.07.009>

- Charnay, B., & Lebonnois, S. (2012). Two boundary layers in Titan's lower troposphere inferred from a climate model. *Nature Geoscience*, 5, 106–109. <https://doi.org/10.1038/ngeo1374>
- Cottini, V., Nixon, C. A., Jennings, D. E., de Kok, R., Teanby, N. A., Irwin, P. G. J., & Flasar, F. M. (2012). Spatial and temporal variations in Titan's surface temperatures from Cassini CIRS observations. *Planetary and Space Science*, 60, 62–71. <https://doi.org/10.1016/j.pss.2011.03.015>
- Coustenis, A., Achterberg, R. K., Bampasidis, G., Jennings, D., Nixon, C., Vinatier, S., et al. (2010). Titan's atmosphere from Cassini-Huygens. In *38th cospar scientific assembly*, 38, pp. 9.
- Fenton, L. K., & Lorenz, R. D. (2015). Dust devil height and spacing with relation to the Martian planetary boundary layer thickness. *Icarus*, 260, 246–262. <https://doi.org/10.1016/j.icarus.2015.07.028>
- Fulchignoni, M., Ferri, F., Angrilli, F., Ball, A. J., Bar-Nun, A., Barucci, M. A., et al. (2005). In situ measurements of the physical characteristics of Titan's environment. *Nature*, 438(7069), 785–791. <https://doi.org/10.1038/nature04314>
- Gillette, D. A., & Sinclair, P. C. (1990). Estimation of suspension of alkaline material by dust devils in the United States. *Atmospheric Environment*, 24, 1135–1142. [https://doi.org/10.1016/0960-1686\(90\)90078-2](https://doi.org/10.1016/0960-1686(90)90078-2)
- Greeley, R., & Iversen, J. D. (1985). *Wind as a geological process on Earth, Mars, Venus and Titan* (Vol. 4). Cambridge, London: Cambridge University Press.
- Greeley, R., Whelley, P. L., Arvidson, R. E., Cabrol, N. A., Foley, D. J., Franklin, B. J., et al. (2006). Active dust devils in Gusev crater, Mars: Observations from the Mars Exploration Rover Spirit. *Journal of Geophysical Research*, 111, E12S09. <https://doi.org/10.1029/2006JE002743>
- Griffith, C. A., Hall, J. L., & Geballe, T. R. (2000). Detection of daily clouds on Titan. *Science*, 290(5491), 509–513. <https://doi.org/10.1126/science.290.5491.509>
- Griffith, C. A., Penteado, P., Baines, K., Drossart, P., Barnes, J., Bellucci, G., et al. (2005). The evolution of Titan's mid-latitude clouds. *Science*, 310, 474–477. <https://doi.org/10.1126/science.1117702>
- Hayes, A. G., Lorenz, R. D., & Lunine, J. I. (2018). A post-Cassini view of Titan's methane-based hydrologic cycle. *Nature Geoscience*, 11(5), 306–313. <https://doi.org/10.1038/s41561-018-0103-y>
- Holton, J. R. (1992). *An introduction to dynamic meteorology*. San Diego: Academic Press.
- Hueso, R., & Sánchez-Lavega, A. (2006). Methane storms on Saturn's moon Titan. *Nature*, 442(7101), 428–431. <https://doi.org/10.1038/nature04933>
- Jackson, B., & Lorenz, R. D. (2015). A multiyear dust devil vortex survey using an automated search of pressure time series. *Journal of Geophysical Research*, 120, 401–412. <https://doi.org/10.1002/2014JE004712>
- Jackson, B., Lorenz, R. D., Davis, K., & Lipple, B. (2018). Using an instrumented drone to probe dust devils on Oregon's Alvord Desert. *Remote Sensing*, 10, 65. <https://doi.org/10.3390/rs10010065>
- Klose, M., Jemmett-Smith, B. C., Kahanpää, H., Kahre, M., Knippertz, P., Lemmon, M. T., et al. (2016). Dust devil sediment transport: From lab to field to global impact. *Space Science Reviews*, 203, 377–426. <https://doi.org/10.1007/s11214-016-0261-4>
- Klose, M., & Shao, Y. (2016). A numerical study on dust devils with implications to global dust budget estimates. *Aeolian Research*, 22, 47–58. <https://doi.org/10.1016/j.aeolia.2016.05.003>
- Larson, E. J. L., Toon, O. B., & Friedson, A. J. (2014). Simulating Titan's aerosols in a three dimensional general circulation model. *Icarus*, 243, 400–419. <https://doi.org/10.1016/j.icarus.2014.09.003>
- Lora, J. M., Lunine, J. I., & Russell, J. L. (2015). GCM simulations of Titan's middle and lower atmosphere and comparison to observations. *Icarus*, 250, 516–528. <https://doi.org/10.1016/j.icarus.2014.12.030>
- Lora, J. M., Tokano, T., Vatant d'Ollone, J., Lebonnois, S., & Lorenz, R. D. (2019). A model intercomparison of Titan's climate and low-latitude environment. *Icarus*, 333, 113–126. <https://doi.org/10.1016/j.icarus.2019.05.031>
- Lorenz, R. D. (2000). Post-Cassini exploration of Titan—Science rationale and mission concepts. *Journal of the British Interplanetary Society*, 53, 218–234.
- Lorenz, R. D. (2011). On the statistical distribution of dust devil diameters. *Icarus*, 215(1), 381–390. <https://doi.org/10.1016/j.icarus.2011.06.005>
- Lorenz, R. D. (2013). The longevity and aspect ratio of dust devils: Effects on detection efficiencies and comparison of landed and orbital imaging at Mars. *Icarus*, 226, 964–970. <https://doi.org/10.1016/j.icarus.2013.06.031>
- Lorenz, R. D. (2014). Vortex encounter rates with fixed barometer stations: Comparison with visual dust devil counts and large-eddy simulations. *Journal of Atmospheric Sciences*, 71(12), 4461–4472. <https://doi.org/10.1175/JAS-D-14-0138.1>
- Lorenz, R. D. (2017). Wind shear and turbulence on Titan: Huygens analysis. *Icarus*, 295, 119–124. <https://doi.org/10.1016/j.icarus.2017.06.010>
- Lorenz, R. D., Balme, M. R., Gu, Z., Kahanpää, H., Klose, M., Kurgansky, M. V., et al. (2016). History and applications of dust devil studies. *Space Science Reviews*, 203(1-4), 5–37. <https://doi.org/10.1007/s11214-016-0239-2>
- Lorenz, R. D., Claudin, P., Andreotti, B., Radebaugh, J., & Tokano, T. (2010). A 3 km atmospheric boundary layer on Titan indicated by dune spacing and Huygens data. *Icarus*, 205(2), 719–721. <https://doi.org/10.1016/j.icarus.2009.08.002>
- Lorenz, R. D., Griffith, C. A., Lunine, J. I., McKay, C. P., & Rennó, N. O. (2005). Convective plumes and the scarcity of Titan's clouds. *Geophysical Research Letters*, 32, L01201. <https://doi.org/10.1029/2004GL021415>
- Lorenz, R. D., & Jackson, B. K. (2016). Dust devil populations and statistics. *Space Science Reviews*, 203, 277–297. <https://doi.org/10.1007/s11214-016-0277-9>
- Lorenz, R. D., Lunine, J. I., Grier, J. A., & Fisher, M. A. (1995). Prediction of aeolian features on planets: Application to Titan paleoclimatology. *Journal of Geophysical Research*, 100(E12), 26,377–26,386. <https://doi.org/10.1029/95JE02708>
- Lorenz, R. D., Turtle, E. P., Barnes, J. W., Trainer, M. G., Adams, D. S., Hibbard, K. E., et al. (2018). Dragonfly: A rotorcraft lander concept for scientific exploration at Titan. *Johns Hopkins APL Technical Digest*, 34, 374–387.
- Lorenz, R. D., Wall, S., Radebaugh, J., Boubin, G., Reffet, E., Janssen, M., et al. (2006). The sand seas of Titan: Cassini RADAR observations of longitudinal dunes. *Science*, 312, 724–727. <https://doi.org/10.1126/science.1123257>
- MacKenzie, S. M., Nunez, J. I., Turtle, E. P., Lorenz, R. D., Horst, S. M., Le Gall, A., et al. (2019). Titan's surface from Dragonfly: Bridging the gap between composition and environment. In *Lunar and planetary science conference*, Lunar and Planetary Science Conference, 50, pp. 2885.
- Méndez Harper, J. S., McDonald, G. D., Dufek, J., Malaska, M. J., Burr, D. M., Hayes, A. G., et al. (2017). Electrification of sand on Titan and its influence on sediment transport. *Nature Geoscience*, 10, 260–265. <https://doi.org/10.1038/ngeo2921>
- Mitchell, J. L. (2008). The drying of Titan's dunes: Titan's methane hydrology and its impact on atmospheric circulation. *Journal of Geophysical Research*, 113, E08015. <https://doi.org/10.1029/2007JE003017>

- Neakrase, L. D. V., Balme, M. R., Esposito, F., Kelling, T., Klose, M., Kok, J. F., et al. (2016). Particle lifting processes in dust devils. *Space Science Reviews*, 203(1-4), 347–376. <https://doi.org/10.1007/s11214-016-0296-6>
- Neakrase, L. D. V., Greeley, R., Iversen, J. D., Balme, M. R., & Eddlemon, E. E. (2006). Dust flux within dust devils: Preliminary laboratory simulations. *Geophysical Research Letters*, 33, L19S09. <https://doi.org/10.1029/2006GL026810>
- Newman, C. E., Kahana, H., Richardson, M. I., Martinez, G. M., Vicente-Retortillo, A., & Lemmon, M. (2019). Convective vortex and dust devil predictions for Gale crater over three Mars years and comparison with MSL-REMS observations. *Journal of Geophysical Research: Planets*, 124, 3442–3468. <https://doi.org/10.1029/2019JE006082>
- Newman, C. E., Richardson, M. I., Lian, Y., & Lee, C. (2016). Simulating Titan's methane cycle with the TitanWRF General Circulation Model. *Icarus*, 267, 106–134. <https://doi.org/10.1016/j.icarus.2015.11.028>
- Obukhov, A. M. (1971). Turbulence in an atmosphere with a non-uniform temperature. *Boundary-Layer Meteorology*, 2, 7–29. <https://doi.org/10.1007/BF00718085>
- Raasch, S., & Franke, T. (2011). Structure and formation of dust devil-like vortices in the atmospheric boundary layer: A high-resolution numerical study. *Journal of Geophysical Research*, 116, D16120. <https://doi.org/10.1029/2011JD016010>
- Radebaugh, J., Lorenz, R. D., Lunine, J. I., Wall, S. D., Boubin, G., Reffet, E., et al. the Cassini Radar Team (2008). Dunes on Titan observed by Cassini Radar. *Icarus*, 194(2), 690–703. <https://doi.org/10.1016/j.icarus.2007.10.015>
- Rafkin, S., Jemmett-Smith, B., Fenton, L., Lorenz, R. D., Takemi, T., Ito, J., & Tyler, D. (2016). Dust devil formation. *Space Science Reviews*, 203(1-4), 183–207. <https://doi.org/10.1007/s11214-016-0307-7>
- Rafkin, S., Lorenz, R. D., Turtle, E., Barnes, J., Trainer, M., Le Gall, A., et al. (2018). DRAGONFLY: In situ exploration of Titan's meteorology. In *Egu general assembly conference abstracts*, EGU General Assembly Conference Abstracts, 20, pp. 19456.
- Rennó, N. O., Burkett, M. L., & Larkin, M. P. (1998). A simple thermodynamical theory for dust devils. *Journal of Atmospheric Sciences*, 55(21), 3244–3252. [https://doi.org/10.1175/1520-0469\(1998\)055<3244:ASTTFD>2.0.CO;2](https://doi.org/10.1175/1520-0469(1998)055<3244:ASTTFD>2.0.CO;2)
- Rennó, N. O., & Ingersoll, A. P. (1996). Natural convection as heat engine: A theory for CAPE. *Journal of Atmospheric Sciences*, 53(4), 572–585. [https://doi.org/10.1175/1520-0469\(1996\)053<0572:NCAAHE>2.0.CO;2](https://doi.org/10.1175/1520-0469(1996)053<0572:NCAAHE>2.0.CO;2)
- Rodriguez, S., Le Mouélic, S., Barnes, J. W., Kok, J. F., Rafkin, S. C. R., Lorenz, R. D., et al. (2018). Observational evidence for active dust storms on Titan at equinox. *Nature Geoscience*, 11, 727–732. <https://doi.org/10.1038/s41561-018-0233-2>
- Savitzky, A., & Golay, M. J. E. (1964). Smoothing and differentiation of data by simplified least squares procedures. *Analytical Chemistry*, 36, 1627–1639.
- Scargle, J. D., Norris, J. P., Jackson, B., & Chiang, J. (2013). Studies in astronomical time series analysis. VI. Bayesian block representations. *Astrophysical Journal*, 764(2), 167. <https://doi.org/10.1088/0004-637X/764/2/167>
- Schaller, E. L., Brown, M. E., Roe, H. G., & Bouchez, A. H. (2006). A large cloud outburst at Titan's south pole. *Icarus*, 182, 224–229. <https://doi.org/10.1016/j.icarus.2005.12.021>
- Schaller, E. L., Brown, M. E., Roe, H. G., Bouchez, A. H., & Trujillo, C. A. (2006). Dissipation of Titan's south polar clouds. *Icarus*, 184, 517–523. <https://doi.org/10.1016/j.icarus.2006.05.025>
- Schröder, S. E., Karkoschka, E., & Lorenz, R. D. (2012). Bouncing on Titan: Motion of the Huygens probe in the seconds after landing. *Planetary and Space Science*, 73, 327–340. <https://doi.org/10.1016/j.pss.2012.08.007>
- Sinclair, P. C. (1973). The lower structure of dust devils. *Journal of Atmospheric Sciences*, 30(8), 1599–1619. [https://doi.org/10.1175/1520-0469\(1973\)030<1599:TLSODD>2.0.CO;2](https://doi.org/10.1175/1520-0469(1973)030<1599:TLSODD>2.0.CO;2)
- Spilker, T. R. (2005). Significant science at Titan and Neptune from aerocaptured missions. *Planetary and Space Science*, 53(5), 606–616. <https://doi.org/10.1016/j.pss.2004.12.003>
- Stull, R. B. (1988). *An introduction to boundary layer meteorology*. Dordrecht, Boston and London: Kluwer Academic Publishers.
- Tokano, T. (2005). Meteorological assessment of the surface temperatures on Titan: Constraints on the surface type. *Icarus*, 173, 222–242. <https://doi.org/10.1016/j.icarus.2004.08.019>
- Tokano, T. (2010). Relevance of fast westerlies at equinox for the eastward elongation of Titan's dunes. *Aeolian Research*, 2, 113–127. <https://doi.org/10.1016/j.aeolia.2010.04.003>
- Tokano, T., Ferri, F., Colombatti, G., Mäkinen, T., & Fulchignoni, M. (2006). Titan's planetary boundary layer structure at the Huygens landing site. *Journal of Geophysical Research*, 111, E08007. <https://doi.org/10.1029/2006JE002704>
- Tratt, D. M., Hecht, M. H., Catling, D. C., Samulon, E. C., & Smith, P. H. (2003). In situ measurement of dust devil dynamics: Toward a strategy for Mars. *Journal of Geophysical Research*, 108(E11), 5116. <https://doi.org/10.1029/2003JE002161>
- Turtle, E. P., Perry, J. E., Hayes, A. G., Lorenz, R. D., Barnes, J. W., McEwen, A. S., et al. (2011). Rapid and extensive surface changes near Titan's equator: Evidence of April showers. *Science*, 331, 1414. <https://doi.org/10.1126/science.1201063>